Nanopore Unzipping of Individual DNA Hairpin Molecules

Jérôme Mathé,* Hasina Visram,* Virgile Viasnoff,* Yitzhak Rabin,[†] and Amit Meller*

*The Rowland Institute at Harvard, Harvard University, Cambridge, Massachusetts, USA; and [†]Department of Physics, Bar-Ilan University, Ramat-Gan, Israel

ABSTRACT   We have used the nanometer scale α-Hemolysin pore to study the unzipping kinetics of individual DNA hairpins under constant force or constant loading rate. Using a dynamic voltage control method, the entry rate of polynucleotides into the pore and the voltage pattern applied to induce hairpin unzipping are independently set. Thus, hundreds of unzipping events can be tested in a short period of time (few minutes), independently of the unzipping voltage amplitude. Because our method does not entail the physical coupling of the molecules under test to a force transducer, very high throughput can be achieved. We used our method to study DNA unzipping kinetics at small forces, which have not been accessed before. We find that in this regime the static unzipping times decrease exponentially with voltage with a characteristic slope that is independent of the duplex region sequence, and that the intercept depends strongly on the duplex region energy. We also present the first nanopore dynamic force measurements (time varying force). Our results are in agreement with the ~log($\dot{V}$) dependence at high $\dot{V}$ (where $\dot{V}$ is the loading rate) observed by other methods. The extension of these measurements to lower loading rates reveals a much weaker dependence on $\dot{V}$.

INTRODUCTION

Many cellular processes, such as DNA replication and RNA transcription, involve the unzipping of double-stranded DNA by proteins (Alberts et al., 1994). The forces and timescales associated with the breakage of the bonds stabilizing the secondary and tertiary structures of nucleic acids can now be studied at the single molecule (SM) level. For example, the unzipping kinetics of double-stranded DNA (dsDNA) and structured RNA molecules such as Ribozymes have been studied using optical "tweezers" and atomic force microscopy (AFM) (Bockelmann et al., 1997; Rief et al., 1999; Strunz et al., 1999; Bustamante et al., 2000; Liphart et al., 2001; Bockelmann et al., 2002). Early measurements have primarily provided the equilibrium thermodynamic properties of the molecules under test. More recent kinetic approaches have been focused on the kinetics of bond breakage under increasing force (or loading rate) (Evans, 2001). These time-dependent kinetics experiments were interpreted in terms of a one-dimensional energy landscape along the direction of the applied force (Evans and Ritchie, 1999; Cocco et al., 2001; Evans, 2001; Lubensky and Nelson, 2002).

SM analysis of biomolecules can reveal information masked by ensemble averaging, such as the variation in the behavior of putatively identical molecules, and short-lived intermediate states. This comes at a price; in the SM approach hundreds of copies of the same molecule must be analyzed, one at a time, to obtain appropriate statistics. Typically, SM force measurements entail the specific immobilization of the DNA or RNA molecule to the force probe at one end, and to a rigid surface at the other. This requirement severely limits the data throughput and complicates the sample preparation. Here we describe an active nanopore-based unzipping method that does not involve the coupling of the test molecules to the force probe. Our method can be used to control the unzipping kinetics of individual DNA hairpins at a constant force as well as at a constant loading rate, with data throughput exceeding ~100 molecules per minute.

Nanopores, and in particular, protein channels such as the bacterial alpha-Hemolysin (α-HL) (Song et al., 1996), have been recently used to obtain information on the length and sequence of single-stranded DNA (ssDNA) and RNA molecules (Kasianowicz et al., 1996; Akeson et al., 1999; Meller et al., 2000, 2001) and to detect the stochastic binding kinetics of different analytes to modified portions of the pore (Howorka et al., 2001). The α-HL pore consists of two main parts: an ~2.5-nm diameter cavity ("vestibule") and an ~1.5-nm diameter channel ("stem"), which permeates the cell membrane (Song et al., 1996). dsDNA domains can be lodged in the 2.5-nm vestibule part but they cannot enter the 1.5-nm channel (the diameter of dsDNA is ~2.2 nm). Recently it has been demonstrated that the closing-opening kinetics of short blunt-ended DNA hairpins (from three to eight basepairs) can be directly measured using the nanopore, by lodging the hairpins in the α-HL vestibule, and detecting the time required for their thermally activated opening (Vercoutere et al., 2001). Upon the spontaneous opening of the hairpin, the ssDNA enters the 1.5-nm channel, causing a brief (but discernable) blockade in the ion current flowing through the pore, thus permitting the detection of the time interval from hairpin lodging to its first opening.

Force-induced unzipping of longer double-stranded helical domains (50 bp) of DNA was recently demonstrated using the α-HL pore (Sauer-Budge et al., 2003). It was found that the

characteristic passage time of the molecules, which includes the sliding of the single strand through the pore, plus their unzipping time, follows an exponential dependence on the applied voltage (in the range 140–180 mV). We note that in this approach a single voltage value was used to control the entry rate of the DNA into the pore and the DNA unzipping kinetics. Since the entry rate sharply decreases with decreasing voltage (Meller and Branton, 2002) (e.g., from ~1 s^{-1} at 120 mV down to 0.01 s^{-1} at 60 mV, measured at a typical DNA concentration of 1 μM), the extension of these measurements to a broader range of voltages, and in particular to voltages <100 mV, is technically impossible. In addition, the exploration of bimolecular bonds under time-varying forces, and in particular the dynamic force spectroscopy of DNA unzipping is highly desirable.

To enable nanopore measurements with time-dependent electric fields, we have recently developed a method that allows us to rapidly change the electric field applied across the nanopore during the passage of the polynucleotide (Bates et al., 2003). In this report we apply this method to study the unzipping kinetics of individual DNA hairpin molecules, over a wide range of voltages from 30 mV to 150 mV and at different loading rates (0.5–100 V/s). Specifically, high voltage was used to optimize the entry rate into the pore, whereas the unzipping voltage was kept variable. Thus, hundreds of individual molecules can be probed over a short period of time (a few minutes). Moreover, our method allows us to perform dynamic force measurements in which a constant loading rate is applied rather than a constant force. These two complementary measurements allow us to resolve small enthalpy changes in the DNA hairpin, down to 1 kcal/mol. We demonstrate our method by an extensive study of the unzipping kinetics of DNA hairpins as a function of voltage.

MATERIALS AND METHODS

PAGE-purified ssDNA and DNA hairpins (Eurogentec, San Diego, CA) were buffered in 10 mM Tris, 1 mM EDTA, pH 8.5 solution and, before the measurements, were heated to 75°C for 10 min and then quenched to 4°C. The hairpin molecules consisted of a 3′ single stranded overhang (50 mer poly-dA), and a 10-bp helical part containing an intervening six base loop with the following sequence (the self-complementary parts are underlined):

HP1 : 5′ − GCTCTGTTGCTCTCTCGCAACAGAGC(A)$_{50}$.

In addition, a similar hairpin (HP2) with a single (TT) mismatch on the fifth base from the 5′ end, was also prepared with the following sequence:

HP2 : 5′ − GCTCTGTTGCTCTCTCGCAACTGAGC(A)$_{50}$,

and also a 7-bp helix hairpin (HP3), with the following sequence:

HP3 : 5′ − GTCGAACTTTTGTTCGAC(A)$_{50}$.

The basic apparatus and experimental method used for reconstituting the α-HL channel in a horizontally supported planar lipid bilayer has been

described previously (Meller et al., 2001). The temperature of the system was maintained at 15.0 ± 0.1°C, using a custom cell design (Bates et al., 2003). The buffer solution was 1M KCl, 10 mM Tris-Hcl, with a pH of 8.5. The α-HL open pore conductance under these conditions was 0.82 nS in the forward bias. The ion current was measured using a patch-clamp amplifier (Axopatch 200B, Axon Instruments, Union City, CA) and the signal was filtered using a 100 kHz low-pass 4-poles Butterworth filter (Krohn Hite 3302, Avon, MA). The signal was digitized at 1 MHz / 12 bits using a DAQ card. All control and acquisition software was written using National Instruments' LabView. Our apparatus incorporates a feedback loop used to control the applied transmembrane voltage, as described earlier (Bates et al., 2003). The response time of the membrane potential to a step in the control voltage was 4 ± 1 μs. In each experiment (performed at given conditions set by the voltage or the voltage ramp) we typically collected over 1000 unzipping events. Our software and hardware combination permits high-throughput unattended data acquisition, such that the total acquisition time for each experiment was ~10 min.

Each unzipping event consisted of three parts: 1), threading and sliding the single-stranded overhang until the helical part was lodged inside the vestibule of the α-HL; 2), holding the hairpin inside the pore at low voltage; and 3), unzipping. The first and the second parts were designed to prepare the system for the third part, such that unzipping always starts at a given configuration of the molecule with respect to the pore. We note that in this experiment, as with any single-molecule experiment, variations between molecules or events are unavoidable. We performed a set of control measurements (described below) and repeated our unzipping experiments many times to reduce data scatter. The unzipping part consisted of two types of measurements: unzipping at stationary force, and unzipping with a fixed loading rate. These experiments are described in the "Results" section.

The voltages and times selected for the first two parts (sliding and holding) were unchanged in all experiments. In Fig. 1 we display the first few milliseconds (ms) of a typical unzipping event performed at a constant force. The upper panel schematically depicts the state of the DNA with respect to the pore at the different stages of the process. The middle panel displays the applied voltage as a function of time and the lower panel is the resulting pore current. The event begins with the threading of the single-stranded poly(dA) end inside the pore. The entry of the polynucleotide into the channel is detected by the abrupt decrease in the open pore current, which sets off a trigger in our acquisition system and defines the $t = 0$ point (left dashed line). The molecule is drawn inside the channel at $V = 120$ mV for a time $t_d = 300 \mu s$. This time was chosen to be slightly larger than the most probable translocation time, t_P, of 40 mer DNA. Note that our hairpins contain a 50 nucleotide (nt) overhang but only 38 nt must translocate through the pore to fully lodge the hairpin inside the pore vestibule because the channel itself can accommodate 12 nt (Meller et al., 2001). Therefore, at $t = t_d$ most of the DNA hairpins are expected to be fully lodged in the α-HL vestibule. This hypothesis was verified by two independent supplementary measurements: in the first experiment we varied t_d (from 50 to 700 μs) and measured the distribution of escape times upon the reversal of the voltage to $V = -120$ mV at $t = t_d$. We observed a monotonic increase in the typical time required for the molecules to be pulled away from the pore for t_d values between 50 and 300 μs. But, for $t_d > 300 \mu$s the curve saturated to a constant level, indicating that the single-strand overhang of DNA was threaded through the channel and then stopped when the double-stranded helical part entered the vestibule (Mathé et al.). Further evidence came from the analysis of the level of the blocked ion current during t_d. We found that the blocked pore current displayed two peaks: a peak at the normal poly(dA) blocked level (~11 pA) (Meller et al., 2000) and a low-current peak at ~6 pA. The lower current peak was attributed to additional blocking of the pore by the helical part of the hairpin occupying the α-HL vestibule.

Note that the fraction of unzipped hairpins at $t = t_d = 300$ μs is very small. We quantify this fraction by measuring the translocation probability distribution of the hairpin molecule at $V = 120$ mV (data not shown). From this distribution we estimate that the fraction of unzipped hairpins at $t = t_d = 300 \mu s$ is smaller than 0.5%. After the initial sliding of the DNA, at
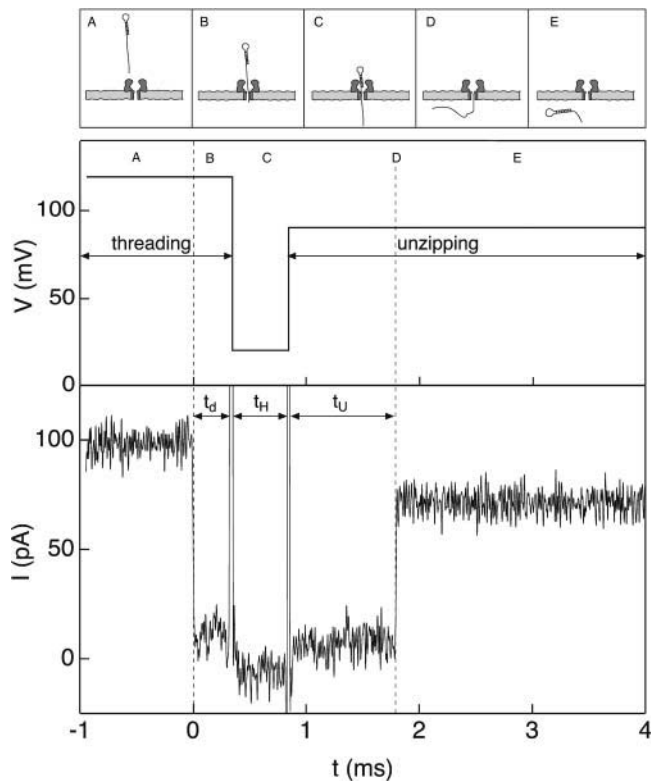
FIGURE 1 (*Top panel*) Cartoon depicting the state of the DNA hairpin with respect to the α-HL pore before and after unzipping. (*A*) The pore is open before the entry of the 3′ single-stranded overhang. (*B*) The ssDNA part enters and slides through the pore driven by the high electric field. (*C*) The hairpin is held at low voltage. (*D*) Unzipping and sliding of the molecule through the pore. (*E*) The pore is cleared. (*Middle panel*) Voltage applied across the pore as a function of time. The entry of the DNA inside the pore triggers the application of the voltage pattern shown at $t = 0$. (*Lower panel*) Pore current as a function of time. At $t = 0$ the DNA enters inside the pore, reducing the ionic current from $\sim$97 pA to $\sim$11 pA. The molecule is drawn inside the pore after its entry for a time $t_d = 0.3$ ms at 120 mV. Then the molecule is held in the pore during $t_H = 0.5$ ms using a voltage, which does not induce unzipping (20 mV). The sharp spikes in the pore current at $t = t_d$ and at $t = t_d + t_H$ result from the abrupt changes in the applied voltage, as shown in the middle panel. Current traces were recorded with 100 KHz filter and sampled at 1 MHz. The data were smoothed with 10 KHz filter for display purposes.

$t = t_d$ the voltage was reduced to a low ''holding'' potential (20 mV) for a time $t_H = 500 \mu s$. This voltage was found to be sufficiently large to keep the hairpins in the vestibule, but was too small to induce significant unzipping as evident from the data displayed below. The choice of 500 μs was dictated by convenience (in a separate set of experiments we held hairpins in the pore for up to 5 s). At the end of the holding period the unzipping voltage, V_U (or the loading rate), $\dot{V} = dV/dt$ was applied.

RESULTS

We discern three consecutive steps in the nanopore unzipping process of the DNA hairpins: A), the entry and sliding of the ssDNA overhang (50 nt), until the double-stranded (helical) part itself is lodged in the 2.5-nm vestibule of the α-HL; B), the unzipping of the helical part; and C),

translocation of the unzipped single-strand part through the pore. We have characterized each of these steps, to resolve their typical timescales at different voltages. We show that using the active voltage control method (see Materials and Methods), the overhang entry (part A) can be decoupled from the other steps, and that the translocation time of the unzipped strands (part C) is much shorter than the typical unzipping time and thus can be neglected.

We first characterize the timescale associated with ssDNA threading in the pore as a function of voltage. We show that the typical timescale for unzipping a 10-bp hairpin is substantially longer than the threading time of the ssDNA. Next, we display the unzipping kinetics information for stationary (or step function) voltages in the range 30–150 mV. This data can be used to determine the effective charge on the DNA strand inside the pore. Finally we display the dependence of the unzipping kinetics on the loading rate. Our data are interpreted using a simple theoretical model similar to the one developed for other SM unbinding experiments (Evans, 2001).

The translocation time distributions of ssDNA

We define the translocation time (t_T) of each individual DNA as the time interval from the entry of the first few bases of the DNA molecule inside the channel part of the α-HL pore, to the exit of the molecule from the other side of the channel. These events are clearly observed by the abrupt reduction of the ionic current flowing through the pore down to $\sim$10% of the open pore current (Meller et al., 2001). In the case of the hairpins, the DNA can only enter the channel with its single-strand 3′ overhang, since the loop at its other end is too large to enter the pore (Vercoutere et al., 2001). In this case, t_T is a sum of the three consecutive processes described above, i.e., $t_T = t_{s1} + t_{unzip} + t_{s2}$, where t_{s1} is the sliding time of the single strand overhang (poly(dA)$_{50}$), t_{s2} is the sliding time of the unzipped hairpin + loop (26 bases), and t_{unzip} is the unzipping time.

In Fig. 2, we display the translocation time distributions of $\sim$1500 events of the poly(dA)$_{90}$ ssDNA. The distribution of the ssDNA displays a prominent peak at $t_p = 0.5$ ms, which was used to characterize the process (Meller et al., 2000, 2001). Our previous studies demonstrated that t_p scales linearly with the number of bases (for 12-mers and above) (Meller et al., 2001). Thus, from the translocation distribution of the poly(dA)$_{90}$ we can estimate $t_{s1} \sim 0.5$ ms $\times$ 50/90 $\sim$ 0.28 ms. Notice that this time is much smaller than the characteristic t_T of the DNA hairpin ($\sim$2–10 ms) measured in a similar way (data not shown). Nevertheless, as is described below, it is possible to decouple the initial sliding from the unzipping process, thus eliminating t_{s1} completely.

The contribution of t_{s2} to the unzipping process can be estimated from our studies of the translocation time of poly(dA) as a function of V (Meller et al., 2001; Bates et al., 2003). Based on these measurements we estimate $t_{s2} \sim 660$
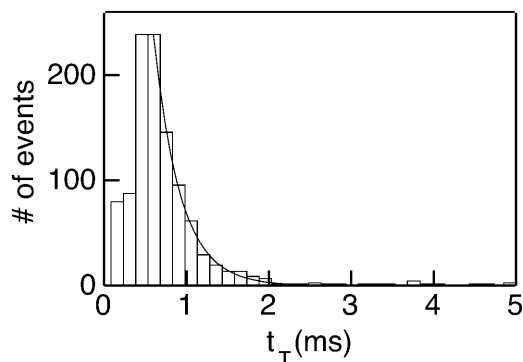
FIGURE 2 Translocation time distribution of an ssDNA (poly(dA)$_{90}$) measured at $V = 120$ mV and 15°C. The histogram was constructed from ~1500 individual events. After $t_T > t_P = 0.5$ ms (the most probable translocation time), the distribution is fitted by a single exponential with a time constant of 0.32 ms.

μs at 30 mV and ~ 100 μs at 150 mV, for 26 nucleotides (see Supplementary Material). The estimated values of t_{s2} as a function of the voltage can be subtracted from the total unzipping time measured in each event to yield a more accurate estimation of t_{unzip}. We note however, that this correction is small (see below) and does not impact our results.

The measurements of t_{s2} also give an idea of the average sliding time per nucleotide (e.g., 6 μs at 100 mV), a timescale that is important for the elucidation of the unzipping mechanism inside the pore. When the hairpin is lodged in the pore its unzipping kinetics is affected by the competition between the rezipping and sliding processes (an unzipped nucleotide can either rejoin the hairpin or slide along the channel, thereby blocking rezipping). If the sliding time is short compared to the rezipping time, rezipping will be prohibited. In contrast, if the sliding time is long, the hairpin will undergo many opening-closing transitions before complete unzipping.

Unzipping kinetics at constant force

We first studied the unzipping of DNA hairpins under a stationary voltage (or force). An abrupt change in the voltage was applied across the nanopore and the unzipping kinetics was measured. Typical voltage and current traces used in this experiment are shown in Fig. 3. Upon the application of the unzipping voltage V_U, the current slightly increased to its proper blocked pore level (see Fig. 1 for a zoom in view of the pore current), and stayed at this blocked level until $t \sim 70$ ms (measured from the application of the unzipping voltage). At this point the current abruptly increased to the open pore current level corresponding to this voltage. Since the sliding time of the unzipped hairpin is too short to be resolved on the timescale of Fig. 3, this transition signals the unzipping moment of the hairpin. The unzipping
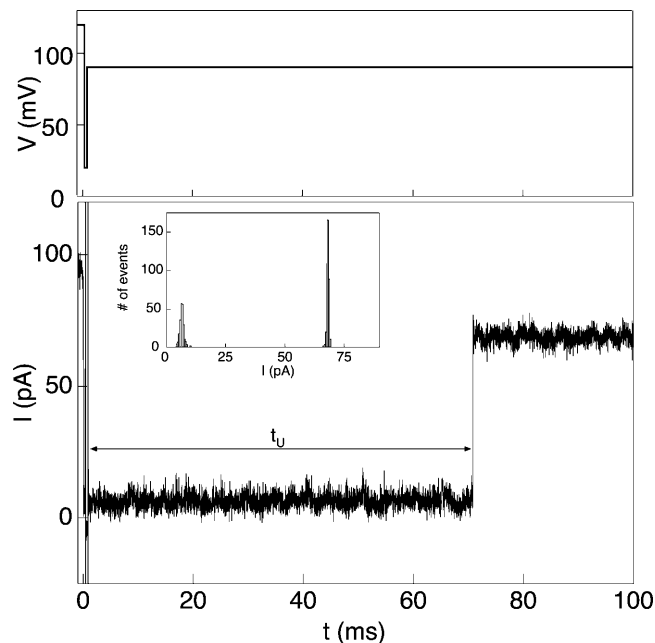

FIGURE 3 Typical unzipping event for the constant voltage experiment. The upper panel displays the applied voltage pattern and the lower panel is the resulting pore current. The DNA enters the channel at time $t = 0$. The molecule is briefly pulled and held in the pore as explained in Fig. 1. At $t = 0.8$ ms, the unzipping voltage is applied (90 mV), but the current is blocked (*lower level*) until unzipping occurs at $t = t_U = 70$ ms, as indicated by the abrupt increase in the current. (*Inset*) Typical distribution of the pore current measured at $t = 5$ ms from ~1000 separate unzipping events. The numbers of events included in the two well-separated peaks can be used to calculate the fraction of unzipped molecules and, therefore, the unzipping probability.

process was repeated using an automated procedure which accumulated ~100 separate unzipping events per minute.

We analyzed our data by calculating the probability that an unzipping event has occurred in the time interval $[0 - t]$, where $t = 0$ is defined as the moment when V_U is applied. For this calculation we acquired ~1000 unzipping events and plotted the average pore current measured in a 50-μs time window centered at time t. The distribution of the currents exhibits two well-separated peaks associated with the blocked and empty pore states respectively (*inset* in Fig. 3). By calculating the ratio of the number of "empty pore" (high-current) events to the total number of events, we obtained the accumulated unzipping probability at time t.

We repeated the measurements described above for different values of V_U (30, 60, 90, 120, and 150 mV) and applied a similar analysis procedure. Our data (the probability to unzip the hairpin as a function of the probing time) are displayed in Fig. 4. At short times (i.e., $t < 1$ ms) the unzipping probability is very small regardless of the amplitude of V_U. At $t \sim 10$ ms we see a pronounced difference between the unzipping probabilities at small and large V_U values. As was discussed earlier, because the unzipping is immediately followed by the translocation of 26 nt (single strand) through the pore, the measured unzipping
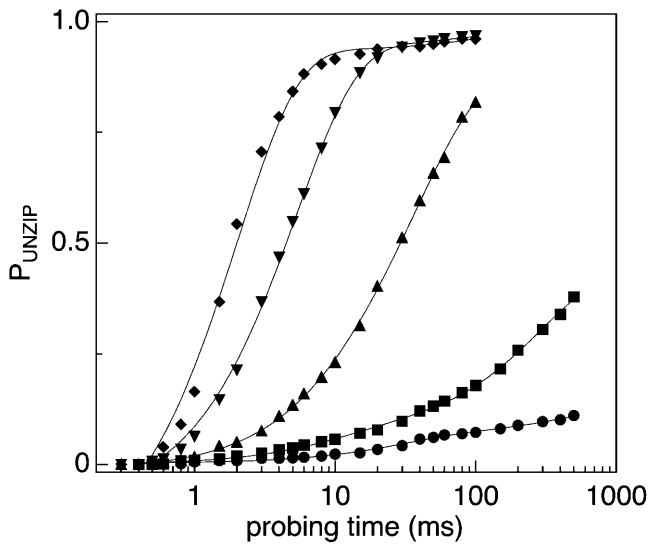
FIGURE 4   The unzipping probability, P_{unzip} as a function of t, for different unzipping voltage levels for HP1. P_{UNZIP} was calculated as the ratio of the number of events under the high current peak to the total number of events (see *inset* of Fig. 3), for each probing time. The voltage levels used: 30 mV (*circles*), 60 mV (*squares*), 90 mV (*triangles*), 120 mV (*inverted triangles*), and 150 mV (*diamonds*). P_{UNZIP} curves were fitted by single exponential functions $P_{UNZIP} = 1 - e^{-t/\tau_U}$ (*solid lines*).
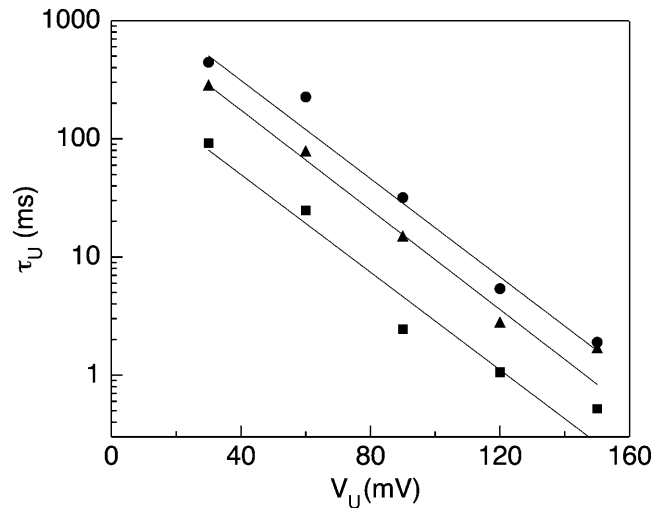

FIGURE 5   The characteristic timescales obtained from the exponential fits of P_{UNZIP} (Fig. 4) as a function of V_U. Data are presented for the perfect match hairpin (HP1, *solid circles*) the single mismatch (HP2, *triangles*), and for the 7-bp hairpin (HP3, *squares*). The data are well approximated by exponential fits (*lines*) yielding an identical slope for the three hairpins with $V_\beta = 22 \pm 2$ mV, and intercept values $\tau_U(0) \sim 2.1 \pm 0.2$ s, 1.2 ± 0.1 s, and 0.34 ± 0.05 s for HP1, HP2, and HP3, respectively.

time includes two terms: the true unzipping time and the sliding time (t_{s2}) of the 26-mer. We corrected our measurements by estimating t_{s2} as explained earlier. However, because the correction is much smaller than the unzipping time ($\sim 1\%$), it had a very small influence on our results.

The unzipping probability distributions shown in Fig. 4 were fit by single exponential functions, which yielded the characteristic unzipping time τ_U, at the different voltage levels. The dependence of τ_U on the unzipping voltage, V_U, is plotted in Fig. 5, for HP1 (*full circles*), HP2 (*triangles*), and HP3 (*squares*), respectively. Notice that τ_U depends exponentially on V_U, as apparent from the straight line fits, and that the exponents in all cases are nearly identical (the lines have nearly identical slopes). We thus fit our data with the function $\tau_U(V_U) = \tau_0 e^{(-V_U/V_\beta)}$. From the fit to the slopes we obtain $V_\beta = 22 \pm 2$ mV, and from the intercepts of the straight lines we get the amplitudes: $\tau_U(0) = 2.1 \pm 0.2$ s for HP1, 1.2 ± 0.1 s for HP2, and 0.34 ± 0.05 s for HP3. Notice, however, that the interpretation of the intercept $\tau_U(0)$ as equilibrium lifetime of the hairpin depends on the assumption that V_β remains independent of the voltage V_U even in the range of low voltages (below 30 mV) that was not studied in our experiment.

The exponential dependence on V is identical to the modified Kramers rate model (Bell, 1978) $\tau_U(V_U) = Ae^{(E_b - Q_{eff}V_U)/k_BT}$, where $\tau_0 = Ae^{E_b/k_BT}$ is the zero voltage transition time, E_b is the energy barrier for dissociation of the hairpin and $-Q_{eff}V_U$ is the reduction in the energy barrier due to the electric field. Thus Q_{eff} has the dimensions of electric charge and $V_\beta = k_BT/Q_{eff}$. From the value of V_β we can estimate

this effective charge $Q_{eff} \approx 1.13 \pm 0.10e$ in the pore. Assuming that this charge is associated with ~ 12 nucleotides that span the α-HL channel (Meller et al., 2001; Vercoutere et al., 2001; Sauer-Budge et al., 2003), the effective charge per nucleotide is: $1.13/12 = 0.094e$.

Unzipping kinetics at constant loading rate

With the active control method, an arbitrary time-dependent voltage $V(t)$ can be applied to measure the dynamics of bond breakage. In particular, force spectroscopy measurements are typically performed at a constant loading rate (Strunz et al., 1999; Evans, 2001), or ramp $\dot{V} = dV/dt$. In the following paragraphs we first show the results of a derivation of the expected distribution of the unzipping voltages for given $\dot{V}$, and the dependence of the critical voltage (or the most probable unzipping voltage) on $\dot{V}$. The detailed derivation is provided in the Supplementary Material. Our analysis follows the approach of Evans and Ritchie (1999), adapted to the nanopore case. We then show that our results are consistent with this simplified model for large loading rates, but deviate from the model at lower rates.

We assume an idealized one-dimensional energy landscape along the direction of the applied force, with a single energy barrier. In equilibrium (with no force applied), the closed hairpin state is represented as a deep minimum in the energy landscape, separated from the open state by an energy barrier E_b. To unzip the hairpin, the molecule has to cross this energy barrier. In the presence of the biasing voltage (or force) the barrier is reduced and the Kramers time (τ_0) is

modified according to $\tau(V) = \tau_0 e^{(-V/V_\beta)}$ where τ_0 and V_β are as defined earlier. We note that here $V = V(t)$ is time dependent. For sufficiently large loading rates rezipping events can be neglected and the probability per unit time that unzipping has occurred between t and $t + dt$ is given by $P(t) = \tau^{-1}(t)\exp\left(-\int_0^t dt'/\tau(t')\right)$. This equation can be expressed in terms of $V(t) = \dot{V}t$, giving us the distribution of the unzipping voltages:

$$P(V) = \frac{1}{\tau_0 \dot{V}}\exp\left[\frac{V}{V_\beta} - \frac{V_\beta}{\tau_0 \dot{V}}\left(\exp\left(\frac{V}{V_\beta}\right) - 1\right)\right]. \quad (1)$$

The critical unzipping voltage, V_C, is defined by the maximum of this distribution, which is:

$$V_C = V_\beta \ln\left(\frac{\tau_0 \dot{V}}{V_\beta}\right). \quad (2)$$

In Fig. 6 we display a typical unzipping event, performed at a constant loading rate of 4.5 V/s. The upper panel depicts the applied voltage and the lower panel shows the pore current. The initial entry of the DNA into the pore was performed as in the previous experiment (i.e., 0.3 ms sliding and 0.5 ms holding of the molecule inside the pore). Upon the application of the voltage ramp, the current remains at the blocked level, but at $t \sim 22$ ms (measured from the beginning of the ramp), the unzipped strand rapidly slides through the pore and we observe a sharp increase in the pore current. From the curve we can directly measure the unzipping voltage, V_U, (130 mV in this case). We note that

the sliding time (t_{s2}) makes the apparent unzipping time (and thus V_U) slightly longer. However, as discussed above, this is a very small effect: in the case displayed here $t_{s2} \sim 0.12$ ms and thus the correction is $0.12/22 = 0.005$, a small fraction of the observed time.

To obtain sufficient statistics we repeated the unzipping experiment at least 1000 times for any given ramp value. A typical distribution of the measured V_U values is given in the inset of Fig. 7. The distribution is well approximated by Eq. 1 (*solid line* in the *inset*). The peak of the distribution is the most probable unzipping force (or the critical voltage, V_C). We repeated our measurements to obtain the dependence of V_C on the voltage ramp in the range 0.5–100 V/s, for HP1, for the hairpin with the single mismatch, HP2, and for HP3 (7-bp helix). Our data are displayed on a semilog plot in Fig. 7 (*circles*, *triangles*, and *squares* for HP1, HP2, and HP3 respectively). At medium and high voltage ramps (5–100 V/s), V_C follows the logarithmic dependence on $\dot{V}$ predicted by Eq. 2. According to Eq. 2, the slope of the straight lines in Fig. 7 is simply V_β. From the logarithmic fit we obtained $V_\beta = 24.7 \pm 1.0$ mV for HP1, 22.5 ± 1.1 mV for HP2, and 23.3 ± 1.9 mV for HP3, in good agreement with the constant voltage measurements described above. As expected from the fact that V_β depends only on the effective charge of DNA inside the pore, all the molecules yielded almost the same slope. Notice that at the lower ramp regime, our data deviates from the simple logarithmic dependence predicted by Eq. 2. This deviation is discussed below. Fit of our data
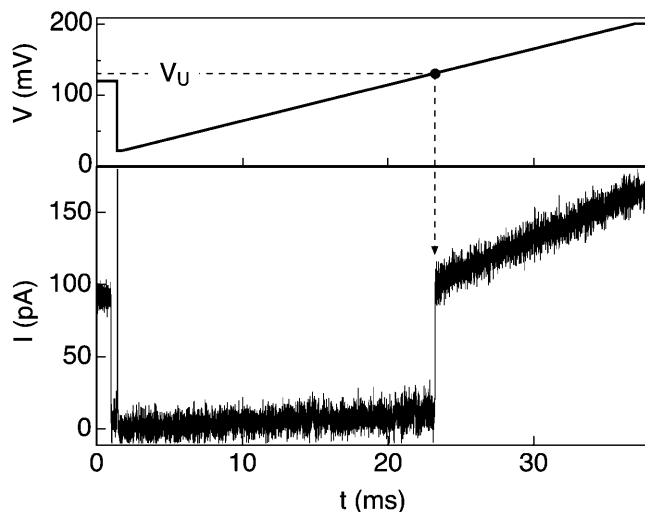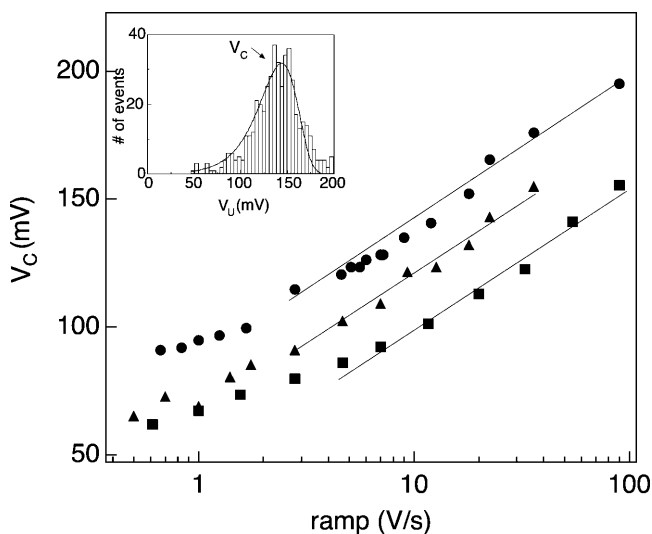

FIGURE 6 Typical unzipping event under constant loading rate. (*Upper panel*) Voltage applied at time $t = 0$, which represents the triggering of the DNA entry into the pore. (*Lower panel*) Pore current during the controlled voltage ramp. The unzipping is readily observable by the jump of current during the ramp of the voltage, from the blocked pore current level to the open pore current level. The unzipping voltage, V_U, is directly obtained from each event.

FIGURE 7 (*Inset*) Collection of ~1500 unzipping events (as in Fig. 6) can be used to obtain the distribution of V_U and the most probable unzipping voltage V_C. The fit to Eq. 1 in the text is shown by the solid line. (*Main figure*) Semilog plot of V_C as a function of the ramp $\dot{V}$, for HP1 (*solid circles*), HP2 (*triangles,*) and HP3 (*squares*). At high ramp values, $V_C \sim V_\beta \log(\dot{V})$, as is apparent from the plots. In this range, we used Eq. 2 to fit the data (*solid lines*), yielding similar slopes for the different molecules of $V_\beta \sim 22$ mV (see text). Notice that at low $\dot{V}$, the data deviates from simple logarithmic dependence (see text).

(for ramp >1.6 V/s) to Eq. 2 yields $\tau_U(0) = 0.72$ s, 0.49 s and 0.17 s for HP1, HP2, and HP3, respectively, values that are smaller than those obtained using the constant voltage method.

DISCUSSION AND CONCLUSIONS

We characterized the ssDNA sliding time from the translocation experiments (see Fig. 2 and Supplementary Material), and performed unzipping experiments of DNA hairpins over a wide range of voltages. We found that the characteristic unzipping time, τ_U, decays exponentially with the unzipping voltage level, V_U (Fig. 5). The slope of the straight lines fits in this figure was found to be independent of the hairpin sequence (and thus their enthalpy), giving a single value $V_\beta = 22 \pm 2$ mV. The amplitudes of the exponential fits provided estimates of $\tau_U(0)$, which were on the order of 1 s.

Previous studies have demonstrated that the dissociation kinetics of short blunt-ended DNA duplexes, lodged in the 2.4-nm α-HL vestibule, can be described as a single-step process, with timescales that correspond to jumps over energy barriers estimated by the free enthalpies of the hairpins calculated in bulk (Vercoutere et al., 2001; Howorka et al., 2001). In these experiments little or no force at all was applied to denature the molecules because blunt-ended DNA duplexes do not enter the α-HL channel portion. The agreement between the dissociation timescales measured in these experiments and in bulk (using mfold; SantaLucia 1998; Zuker 2003), suggested that hairpins' stability was not significantly altered by possible DNA-protein or electrostatic interactions. In contrast, in the current experiments, and in other recent studies (Sauer-Budge et al., 2003; Nakane et al., 2004), single-stranded overhangs extending one end of the DNA hairpins were threaded inside the channel, thus biasing the hairpins' kinetics, presumably by applying force on that strand. Therefore it is not surprising that the typical unzipping times measured in our experiments are significantly shorter than the dissociation times measured using blunt-ended DNA ($\sim 10^2$ s for seven-base duplex), and are similar to the more recent nanopore unzipping experiments mentioned above.

For voltages $>\sim 30$ mV (Fig. 5) or for voltage ramp values $>\sim 4$ V/s (Fig. 7), our data agree with a simple two-state picture in which the energy barrier is lowered by an amount $Q_{eff}V$ in the presence of the electric field. This approximation yielded the same V_β value for the two independent experiments (22 $\pm$ 2 mV for stationary force and 23 $\pm$ 2 mV for the constant ramp). We used these values to estimate the effective charge on the ssDNA inside the 1.5-nm α-HL channel and obtained $1.13e$ for the strand inside the pore or $0.094e$ per nucleotide. (In interpreting Q_{eff} as the effective DNA charge, we implicitly assume that the characteristic length scale associated with barrier to unzipping is of the order of the pore length.) This relatively small value indicates that the negative charge of the DNA in the channel is effectively counterbalanced by "condensation" of positively charged potassium ions and by the presence of polar groups on the inner walls of the α-HL channel, in agreement with previous results (Sauer-Budge et al., 2003), as well as with recent molecular dynamics simulations (Y. Rabin and M. Tanaka, unpublished). Since the counterion distribution in the pore can be affected by electric fields (e.g., the electric field used to draw the ssDNA in the pore also produces an ion current), it is plausible to assume that the effective charge will depend on the voltage. The observation of a voltage-independent effective charge at voltages exceeding 30 mV suggests that this dependence saturates at the observed value of Q_{eff}. More elaborate calculations and measurements are needed to estimate the effective charge for small voltages, and in particular <30 mV.

The dynamic force measurements (Fig. 7) concur with the simple two-state picture described above. At high loading rates (ramp >4 V/s) the unzipping time (and thus V_C) is determined by the rapid change in the potential barrier height due to the force. In this limit the system does not undergo many opening-closing transitions and V_C is directly proportional to $\log(\dot{V})$. For small values of $\dot{V}$ we observe a soft crossover to another regime, characterized by weak dependence of the critical voltage on the loading rate. In this regime the voltage remains sufficiently low for long enough time to allow the system to fluctuate between closed and open states, before the eventual unzipping. An extension to the simple two-state picture presented above to include this effect can be made based on a similar analysis performed for the mechanical unbinding kinetics (Evans and Williams, 2002). We leave this analysis for a future publication.

In summary, combining a nanopore with an active voltage control technique permits the detection of hundreds of individual DNA or RNA molecules in a time-efficient manner, without the need to attach the molecules to a surface, or to a force probe. The ability to independently control the entry process inside the pore and the unzipping process allowed us to investigate the unzipping kinetics in a voltage range that was inaccessible so far, and to apply time-varying forces to DNA hairpins using the nanopore. Because we can access a broad range of voltages and voltage ramps, our measurements may be used to extend the range of unzipping forces accessible to other techniques (used to study DNA and RNA unzipping kinetics), much below the critical dsDNA-ssDNA transition (~ 12 pN; Cocco et al., 2001), and to lower loading rates. However, a better understanding of electrodynamics of the DNA-ions-pore system is required, especially at the low voltage range (<30 mV), where nontrivial dependence of the effective charge on V is expected. The elucidation of the nanopore unzipping kinetics of individual DNA hairpins sets the stage for further studies involving multiple hairpin domains in ssDNA and RNA, and eventually will permit the examination of secondary and tertiary structure in complicated polynucleotides, such as ribozymes.

SUPPLEMENTARY MATERIAL

An online supplement to this article can be found by visiting BJ Online at http://www.biophysj.org.

REFERENCES

Akeson, M., D. Branton, J. Kasianowicz, E. Brandin, and D. Deamer. 1999. Microsecond timescale discrimination among polycytidylic acid, poly-adenylic acid, and polyuridylic acid as homopolymers or as segments within single RNA molecules. *Biophys. J.* 77:3227–3233.

Alberts, B., D. Bray, J. Lewis, M. Raff, K. Roberts, and J. D. Watson. 1994. Molecular Biology of the Cell. Garland Publishing, New York.

Bates, M., M. Burns, and A. Meller. 2003. Dynamics of DNA molecules in a membrane channel probed by active control techniques. *Biophys. J.* 84:2366–2372.

Bell, G. I. 1978. Models for the specific adhesion of cells to cells. *Science.* 200:618–627.

Bockelmann, U., B. Essevaz-Roulet, and F. Heslot. 1997. Molecular stick-slip motion revealed by opening DNA with piconewton forces. *Phys. Rev. Lett.* 79:4489–4492.

Bockelmann, U., P. Thomen, B. Essevaz-Roulet, V. Viasnoff, and F. Heslot. 2002. Unzipping DNA with optical tweezers: high sequence sensitivity and force flips. *Biophys. J.* 82:1537–1553.

Bustamante, C., S. B. Smith, J. Liphart, and D. Smith. 2000. Single-molecule studies of DNA mechanics. *Curr. Opin. Struct. Biol.* 10:279–285.

Cocco, S., R. Monasson, and J. F. Marko. 2001. Force and kinetic barriers to unzipping of the DNA double helix. *Proc. Natl. Acad. Sci. USA.* 98:8608–8613.

Evans, E. 2001. Probing the relation between force-lifetime and chemistry in single molecule bonds. *Annu. Rev. Biophys. Biomol. Struct.* 30:105–128.

Evans, E., and K. Ritchie. 1999. Strength of a weak bond connecting flexible polymer chains. *Biophys. J.* 76:2439–2447.

Evans, E., and P. Williams. 2002. Dynamic force spectroscopy. *In* Physics of Biomolecules and Cells. H. Flyvberg, F. Julicher, P. Ormos, and F.

David, editors. Ecole des Houches d'Ete, LXXV. EDP Sciences, Springer-Verlag, Berlin. 145–185.

Howorka, S., L. Movileanu, O. Braha, and H. Bayley. 2001. Kinetics of duplex formation for individual DNA strands within a single protein nanopore. *Proc. Natl. Acad. Sci. USA.* 98:12996–13001.

Kasianowicz, J., E. Brandin, D. Branton, and D. Deamer. 1996. Characterization of individual polynucleotide molecules using a membrane channel. *Proc. Natl. Acad. Sci. USA.* 93:13770–13773.

Liphart, J., B. Onoa, S. B. Smith, I. Tinoco, Jr., and C. Bustamante. 2001. Reversible Unfolding of Single RNA Molecules by Mechanical Force. *Science.* 292:733–737.

Lubensky, D. K., and D. R. Nelson. 2002. Single molecule statistics and the polynucleotide unzipping transition. *Phys. Rev. E.* 65:031917–1.

Meller, A., and D. Branton. 2002. Single molecule measurements of DNA transport through a nanopore. *Electrophoresis.* 23:2583–2591.

Meller, A., L. Nivon, E. Brandin, J. Golovchenko, and D. Branton. 2000. Rapid nanopore discrimination between single polynucleotide molecules. *Proc. Natl. Acad. Sci. USA.* 97:1079–1084.

Meller, A., L. Nivon, and D. Branton. 2001. Voltage-Driven DNA Translocations through a Nanopore. *Phys. Rev. Lett.* 86:3435–3438.

Nakane, J., M. Wiggin, and A. Marziali. 2004. A nanosensor for transmembrane capture and identification of single nucleic acid molecules. *Biophys. J.* 87:615–621.

Rief, M., H. Clausen-Schaumann, and H. E. Gaub. 1999. Sequence-dependent mechanics of single DNA molecule. *Nat. Struct. Biol.* 6:346–349.

SantaLucia, J. 1998. A unified view of polymer, dumbbell, and oligonucleotide DNA nearest-neighbor thermodynamics. *Proc. Natl. Acad. Sci. USA.* 95:1460–1465.

Sauer-Budge, A. F., J. A. Nyamwanda, D. K. Lubensky, and D. Branton. 2003. Unzipping kinetics of double-stranded DNA in a nanopore. *Phys. Rev. Lett.* 90:238101.

Song, L., M. R. Hobaugh, C. Shustak, S. Cheley, H. Bayley, and J. E. Gouax. 1996. Structure of staphylococcal α-hemolysin a heptameric transmembrane pore. *Science.* 274:1859–1865.

Strunz, T., K. Oroszlan, R. Schäfer, and H.-J. Güntherodt. 1999. Dynamic force spectroscopy of single DNA molecules. *Proc. Natl. Acad. Sci. USA.* 96:11277–11282.

Vercoutere, W. A., S. Winters-Hilt, H. Olsen, D. Deamer, D. Haussler, and M. Akeson. 2001. Rapid discrimination among individual DNA hairpin molecules at single-nucleotide resolution using an ion channel. *Nat. Biotechnol.* 19:248–252.

Zuker, M. 2003. Mfold web server for nucleic acid folding and hybridization prediction. *Nucleic Acids Res.* 31:3406–3415.